Biological Hair-Inspired AgNWs@Au-Embedded Nafion Electrodes with High Stability for Self-powered Ionic Flexible Sensors

Chun Zhao[a, ‡], Yanjie Wang[a, ‡ *], Gangqiang Tang[a], Yujun Ji[a], Xin Zhao[a], Dong Mei[a], Jie Ru[a], Longfei Chang[b], Bo Li[c], Denglin Zhu[a], and Lijie Li[d]

[a] *Jiangsu Provincial Key Laboratory of Special Robot Technology, Hohai University, Changzhou campus, Changzhou, 213022, China*

[b] *Anhui Province Key Lab of Aerospace Structural Parts Forming Technology and Equipment, Hefei University of Technology, Hefei, 230009, China.*

[c] *School of Mechanical Engineering, Xi'an Jiaotong University, Xi'an, Shaanxi 710049, China.*

[d] *College of Engineering, Swansea University, Swansea, SA1 8EN, UK*

Abstract: Ionic flexible sensors (IFS) usually consist of an ionomer matrix and two conductive electrodes, the failure of which mostly origins from interfacial debonding between matrix and electrode layers. To improve electrode's adhesion and impedance matching with matrix, polymer binder or plasmonic heating technology is used to enhance the adhesion of electrodes, but there are technical challenges such as high resistance and harsh condition. Herein, inspired by biological hair, we proposed a reliable and facile method to form AgNWs@Au-embedded Nafion flexible electrodes (AN FEs) for IFS without rigorous temperature and harsh condition. Through integrating the spraying and electrodepositing Au method, we achieved that the AgNWs are partly embedded in the matrix layer for forming the embedded layer, similar to the root of biological hair, which is used to fix the FEs and collect the ion charges. The other parts of AgNWs exposed on the surface form the conductive mesh layer for transmitting the signal, analogous to the tip of biological hair. Compared with other AgNWs FEs, AN FEs exhibit high adhesion (~ 358 KPa) and low sheet resistance (~ 3.7 Ω/□), and high stabilities after 100 washing cycles, 200s H_2O_2 corrosion or 1500s HCl corrosion. A self-powered IFS prepared by AN FEs can achieve dual sensing of mechanical strain and ambient humidity, and still has promising sensing performance after being exposed to air for 2 months, which further indicates potential application of the prepared FEs in next-generation multifunctional flexible electronic devices.

Keywords: ionic flexible sensor, bio-inspired electrode, silver nanowires (AgNWs), Nafion, adhesion, resistance, robustness

1. Introduction

Over the past few decades, IFS inspired by natural perception ability of humans have attracted considerable attention from researchers and are being developed rapidly. Compared to conventional rigid sensors, IFS exhibit distinct properties such as deformability, super-hydrophilicity and biocompatibility, and have shown broad application prospects in fields such as medical monitoring, human-interactive technologies and electronic skins. As one of the key elements in the IFS for collecting ion charges and transmitting signal, FEs are facing a new challenge, that is, being flexible and stable [1-6]. Standard FEs are typically prepared by sputtering indium tin oxide (ITO) thin films with excellent electrical conductivity. However, researchers are looking for alternatives to ITO due to the facts that ITO films are too brittle to meet the demands for next generation flexible electronics. In the past decade, carbon nanotubes, grapheme, solution-processed metal nanowire (NW) networks and poly (3, 4-ethylenedioxythiophene): polystyrene-sulfonate (PEDOT: PSS) have been used as FEs [7-13]. Among them, silver nanowires (AgNWs) are used widely, which not only exhibit the electrical and thermal conductivity, and mechanical flexibility [14], but also can be dispersed in some solvents as an ink and printed or coated on different flexible matrices at room temperature to realize low-cost and high throughput production of FEs [15, 16].

Although considerable efforts have been made to develop some AgNWs FEs with promising flexibility and stability, a series of challenges still hinder the application of AgNW FEs in the flexible sensors. First, the poor adhesion between the AgNWs FEs and the matrix deteriorates the electrical and mechanical stability of the fabricated sensors and reduces effective electrical area, since the AgNWs dispersed in the solvent is loosely deposited on the

surface of the matrix. Recently, some researchers have tried to enhance the adhesion by surface modification, encapsulation using a thin layer of polymer, fast photonic sintering technique, inverted layer processing method and thermal pressing [17, 18]. However, since the interaction between the FEs and the matrix is still by the poor Van der Waals forces, the adhesion is limited. Washing or repeated touch could destroy the electrode layer. However, burying the nanowires in the surface of a polymer is a kind of effective ways [19, 20]. Kim et al. used an inverted layer processing method to bury the AgNWs into the surface of a polymer to enhance the adhesion. Zhang et al. used a high-intensity pulsed light (HIPL) technique to fabricate transparent electrodes with dense Cu@Ag alloy nanowires embedded in the stretchable substrates. It was observed that nanowires were embedded into the soft surface of the polymer matrix to achieve strong adhesion [21]. In addition, the conductivity of AgNWs FEs depends on the effective point contact at nanowire-nanowire junctions. Many as-prepared nanowire FEs that only relies on Van der Waals force to contact each other suffer from poor conductivity due to the weak contact at the junctions. To enhance the stability and conductivity of AgNWs FEs, a series of work have been developed to improve the wire-wire contact [22-26], including thermal welding, mechanical pressing, plasmonic welding, cold welding and electrochemical coating. However, those mentioned methods often have many shortcomings. For example, thermal welding requires a precise control over heating temperature and time to avoid the oxidation of nanowires, and mechanical pressing may damage some inherent structures or the active layer.

As shown in Figure 1a, the bio-hair structure is composed of three functional layers macroscopically, including hair shaft layer, hair root embedded layer, and skin layer. The hair

roots are buried in the skin for forming the hair root embedded layer, which allow the hair to survive during manipulation tasks that involve complex mechanical modes such as stretching, shear, and compression. The hair shafts are exposed on the surface of the skin to form the hair shaft layer, which are used to maintain body temperature and protect the skin. Here, inspired by the structure of biological hair, we proposed a facile, rapid and efficient method to form the AN FEs with high stability without rigorous temperature and harsh condition. Similar to the bio-hair structure, the AN FEs also have three functional layers, including matrix layer, AgNWs embedded layer, and AgNWs@Au layer. In this work, we used the Nafion/ N, N-dimethylacetamide (DMAC) solution to form the matrix layer similar to the skin layer. Then the AgNWs are partly embedded in the matrix layer by the anhydrous ethanol (EtOH) to form the AgNWs embedded layer, similar to the root of biological hair, which are used to fix the FEs and collect the ion charges. The other parts of the AgNWs are exposed on the surface, analogous to the hair shaft layer, which are used to transmit the sensing signal. Meanwhile, Au protective shell and the firm joints between AgNWs are formed by impregnation-electroplating (IEP) process. The prepared FEs by this method exhibit strong adhesion, and can withstand repeated damage to sandpaper and repeated cleaning in deionized (DI) water. Additionally, the conductivity of the prepared FEs remained stable in a strong oxidizing or acid environment for a long time. Moreover, we also prepared a self-powered IFS with the AN FEs, which can not only have dual sensing function, including mechanical strain sensing and humidity gradient sensing (IFS prepared by the AgNWs FE can only realize humidity gradient sensing), but also still has promising sensing performance after being exposed to air for 2 months.

2. Results and discussion

Figures S1a and S1b show the corresponding schematic and the micromorphology of AgNWs FEs. As described in Section 1, AgNWs are loosely stacked on the surface of the ionomer film, which result in the electrode being prone to delamination or shedding when scratched or pressed. In addition, AgNWs are stacked each other only by gravity and Van der Waals force, which cause a weak contact at the wire-wire junctions. When subjected to mechanical deformation, the loosely stacked nanowires would easily move relative to each other, leading to deteriorated conductivity. As shown in Figure S1c, polymers (e.g., Nafion and PDMS) are used as binders to enhance the adhesion of dispersed electrodes. For example, the Nafion/AgNWs mixture is deposited on the surface of the membrane, or the polymer is deposited on the surface of the AgNWs electrode. However, polymers are usually electrically nonconductive, which wrap around the surface of AgNWs, greatly increasing the electrical resistance of the dispersed electrode (Fig. S1d). Recently, we found that the solidified Nafion can be melted again under the action of organic solvent, which have the potential to solve these technical challenges by developing AN FEs. Inspired by biological hair (Fig. 1a), AN FEs studied in this work also have three functional layers, including matrix layer, AgNWs embedded layer for fixing the FEs and collecting the ion charges, and AgNWs@Au layer for transmitting the signal (Fig. 1i), which correspond to the skin layer, the hair root embedded layer, and the hair shaft layer of the bio-hair structure, respectively.

Figure 1b~h shows the preparation process of the AN FEs. The first step is to roughen the surface of the ionomer membrane. This step involves sandblasting to produce a large number of undercuts and grooves on the surface of the membrane, which can increase surface

roughness of the membrane. The second step, i.e., Nafion/DMAC spraying step as initial activation, is to form a matrix layer on the surface of the ionomer membrane, as shown in Figure 1b. In this step, Nafion/DMAC solution is first sprayed onto the surface of the membrane. The undercuts and grooves on the surface of ionomer membrane are filled with the Nafion/DMAC solution with good fluidity and infiltration, which can increase the density of contact points between the matrix layer and the ionomer membrane. After thermos-curing, DMAC and other solvents are evaporated, and the matrix layer changes from liquid to solid, as shown in Figure 1d and 1e. The third step, i.e., AgNWs/EtOH spraying step as main activation, is to form an AgNWs-embedded Nafion electrode on the surface of the matrix layer, as shown in Figure 1c. In this step, AgNWs/EtOH solution is sprayed onto the surface of the matrix layer. The surface of the solidified matrix layer will melt as a result of EtOH, and present a viscous molten state. Therefore, AgNWs can be partly embedded in the melting layer under the action of speed and gravity for forming the AgNWs embedded layer, which is very important for improving the ion storage capacity and stability of electrodes [4]. In addition, the other parts of the AgNWs are incompletely wrapped by the Nafion polymer, and exposed on the surface of the matrix layer, which is beneficial to transmitting the signal, as shown in Figure 1f. After thermos-curing, the EtOH is evaporated, and the surface of the matrix layer changes from molten state to solid, which causes the AgNWs embedded in the melting layer to be fixed, as shown in Figure 1g. It is worth noting that the content of AgNWs exposed on the surface of the matrix depends on the amount of AgNWs used per square centimeter, as shown in Figure S2. The fourth step (IEP process) is to electrodeposit Au onto AgNWs exposed on the surface of matrix layer by electroplating at a room temperature under

the voltage of 3.5 V, as shown in Figure 1h. During the IEP process, Au^{+} in the solution would be reduced to Au atoms, which are selectively deposited onto AgNWs exposed on the surface. Additionally, it is necessary to control the IEP time for improving the performance of AN FEs. When IEP time was 50s, Au atoms filled the gaps among AgNWs and tightly welded them together, which improved the conductivity of the electrodes, as shown in Figure S3.

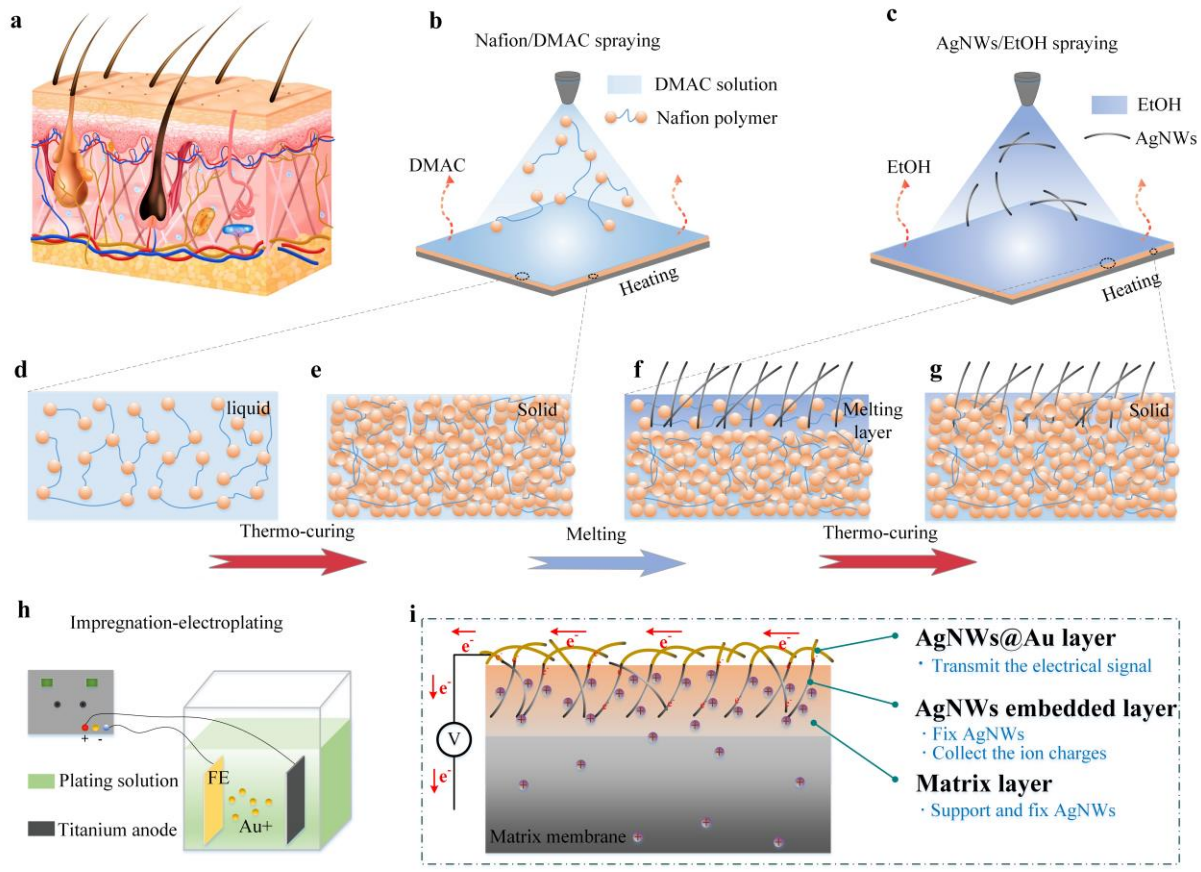

Fig.1. The preparation process of the AN FEs. (a) The structure of the biological hair. (b-h) Schematic illustration showing the fabrication of the AN FEs by integrating the spraying (b, c) and electrodepositing Au method (h). (d) The corresponding schematic of the matrix layer before DMAC volatilizing. (e) The corresponding schematic of the matrix layer before thermos-curing. (f) The surface of the matrix layer presents a viscous molten state, and AgNWs are partially embedded in the

matrix layer. (g) After thermos-curing, AgNWs are embedded into the matrix and fixed. (i) The corresponding schematic of AN FEs.

Figure 2a shows the macromorphology evolution of AN FEs from bare Nafion to conductive one. Figure 2b shows the micromorphology and sheet resistance of AN FEs with 0.2 mg/cm^2 AgNWs. Remarkably, after IEP, the sheet resistance of AN FEs can be reduced from 180.7 Ω/□ to 3.7 Ω/□, which is mainly attributed to the welding connection of AgNWs after IEP. Figure 2c shows the cross-section of AN FEs. The highlighted part represents the AN FEs, and the black part with the ripples is the ionomer film. The thickness of AN FEs is ~6 μm. It can be clearly observed that the undercuts and grooves on the surface of the membrane were filled by the matrix layer, and there are no gaps between the matrix layer and the membrane. To show the embedded structure of AN FEs more clearly in SEM image, AN FEs with lower density of AgNWs were used. Figure 2d shows the micromorphology of AN FEs with 0.12 mg/cm^2 AgNWs. The grey part represents the matrix layer. It can be clearly observed that slim one end of nanowire presents grey and is firmly embedded in the matrix layer, similar to the root of biological hair, which is used to fix the FEs and increase the contact area of the interfacial layers. Meanwhile, the other thick end of nanowire presents highlight and is exposed on the surface of the matrix layer and overlapped with each other, similar to the tip of biological hair, which is used to transmit the sensing signal. Compared with the AgNWs FEs, this structure effectively enhances the adhesion of FEs and reduces the sheet resistance. In addition, AgNWs are uniformly embedded in the matrix layer, which can greatly increase the penetration depth of FEs for enhancing the ion storage capacity of electrodes, thereby improving the response voltage of IFS, as shown in Figure 2e.

Furthermore, it can be found that after electrodepositing Au, the diameter of AgNWs exposed on the surface of the matrix layer is significantly larger than AgNWs embedded in the matrix layer, because the former was wrapped by a layer of Au protective shell. Compared with the Figure S1b, before coating Au shell, clear and continuous edges of each AgNWs were observed. After electrodeposition, the edges disappeared at the junction, indicating the Au atoms were filled in the gap at nanowire-nanowire junctions and welding them together, which greatly improves the sheet conductivity and stability of AN FEs.

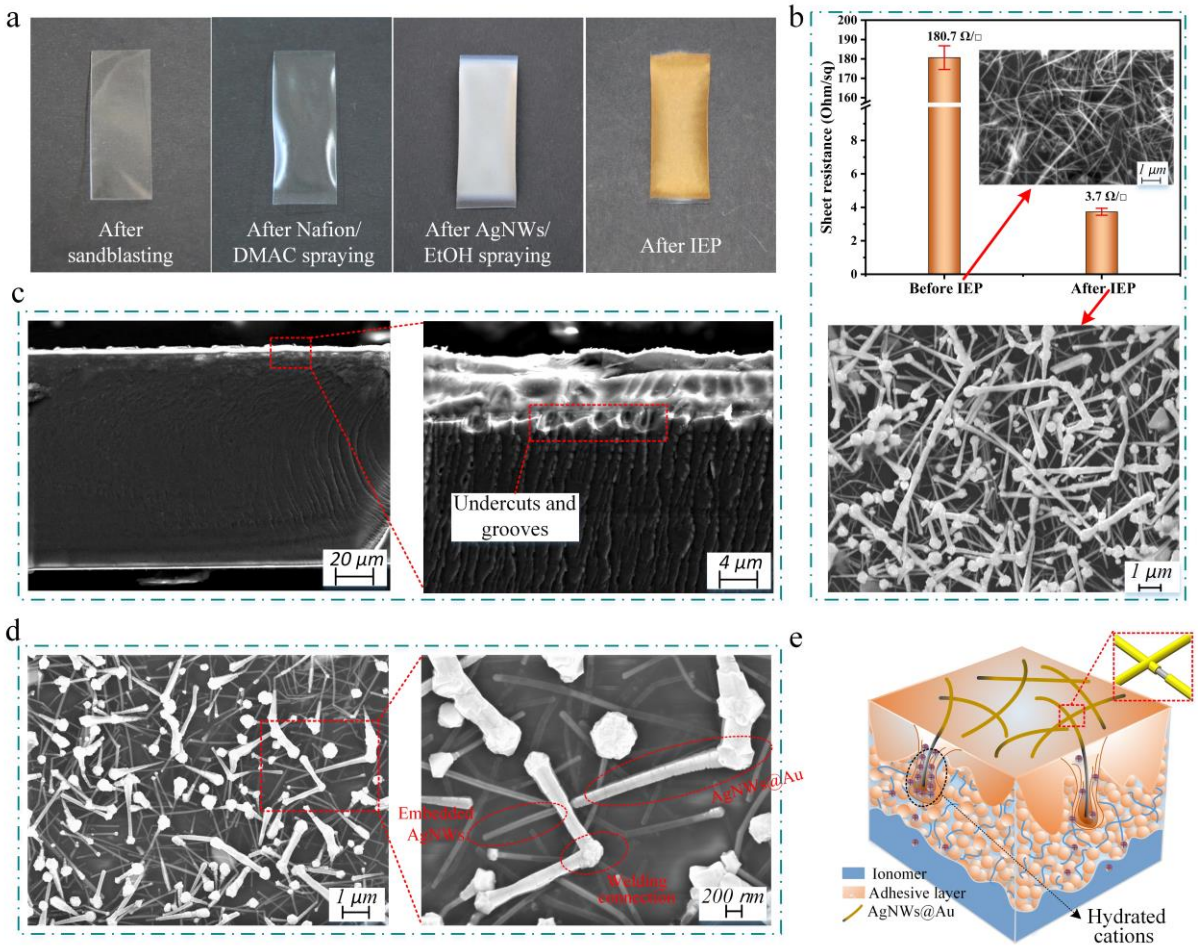

Fig.2. The characterization of AN FEs. (a) The macromorphology of AN FEs. (b) The micromorphology and sheet resistance of AN FEs with 0.2 mg/cm^2 AgNWs before and after IEP. (c) The cross-section of AN FEs. (d) The micromorphology of AN FEs with 0.12 mg/cm^2 AgNWs. (e)

The corresponding schematic of AN FEs.

To further confirm the adhesion performance of AN FEs, we tested its wear resistance and the adhesion. Figure 3a shows the sheet resistance change of FEs after polished by 1500P sandpaper under different pressures (7.5 KPa increments each time from 12.5 KPa to 275 KPa, sanding once per pressure). It is showed that the sheet resistance of AgNWs FEs increases sharply. When the pressure only increases to 50 KPa (5 sanding cycles), the sheet resistance is as high as 2558 Ω/□. This could be attributed to the loose stack of AgNWs each other only by gravity and Van der Waals force, which result in the electrode being prone to delamination or shedding. Compared with AgNWs FEs, AN FEs show excellent stability. When the pressure gradually increases from 12.5 KPa to 200 KPa (25 sanding cycles), the sheet resistance only increases to 112 Ω/□. Even when the pressure increases to 275 KPa (35 sanding cycles), the sheet resistance remains within 600 Ω/□. This satisfactory performance is mainly attributed to the embedded structure similar to biological hair, which makes AgNWs firmly fixed in the matrix layer. Meanwhile, Au protective shell effectively enhances the wear resistance of AgNWs exposed on the surface of the matrix layer due to the fact that after IEP, the AgNWs are connected and welded together to form a whole, and it is difficult to partially peel off. In addition, the Au protective shell greatly increases the diameter of AgNWs exposed on the surface of the matrix layer, preventing it from disconnecting easily after polished, as shown in Figure 2b and Figure 2d. Figure 3b shows the adhesion of AN FEs. Compared with the AgNWs FEs, the adhesion between AN FEs and ionomer membrane is at least several orders of magnitude higher, reaching 358 KPa.

Wearable electronics is one of the important applications of IFS. Therefore, the IFS

needs to be cleaned for being harmless to the human body. To prove the good resistance to water washing of the AN FEs, the ionomer membranes with different FEs were exposed to repeated washing cycles, in which FEs needed to sequentially experience rinsing, rubbing, and crumpling in the DI water. Figure 3c shows that the sheet resistance of AgNWs FEs increased by 24 times after one wash. After 4 washes, AgNWs FEs were completely destroyed and lost conductivity. On the contrary, the sheet resistance of AN FEs was almost constant. After 100 washing cycles, the resistance increased by only 14.6% (from 4.98 Ω to 5.71 Ω), indicating its high reliability during washing. The reason is that the matrix layer fills the undercuts and grooves on the surface of the ionomer membrane and penetrates into it, so that the matrix layer and the ionomer membrane are integrated. To proves this phenomenon, we further performed an additional experiments for visualization (Video S1). In the video, AgNWs FEs had obvious large-area peeling off after one wash, and the sheet resistance of which increased by several orders of magnitude, while the AN FEs remained intact. When used as a strain sensor, the IFS need to have the ability to be immersed in DI water for a long time to maintain the water content of the sensors. Figure 3d shows the surface of FEs before and after immersion in DI water for 24 h, respectively. The AgNWs FEs had obvious peeling off, while the AN FEs remained intact without any peeling phenomenon. As shown in Fig. 3e, compared with AgNWs FEs and Nafion/AgNWs FEs, AN FEs not only have extremely low sheet resistance, but also exhibit excellent adhesion.

The chemical corrosion resistance is also a key assessment for the long-term application of the IFS. Improvement in chemical stability by electrodepositing Au shell is valid even in the highly corrosive environment. As an extreme example for oxidative corrosion, the H_2O_2

was spraied onto the surface of whole FEs. As shown in Figure 3f and Video S2, the resistance of AgNWs FEs without Au protection increased rapidly. In contrast, the Au shell successfully prevented the AgNWs from being corroded by H_2O_2. After bearing 200s corrosion, the resistance still remained stable. The SEM images also confirmed the protective effect of the Au shell, as shown in the inset image. The AgNWs are almost completely disconnected, and only some residues were observed. Conversely, complete AN FEs morphology still existed. Figure 3g shows the sheet resistance in a strong acid corrosion environment. Although the electrical conductivity of AgNWs FEs remained constant before 300s, the resistance increased rapidly after 300s. The reason is that AgNWs are gradually corroded, and there is no fracture in the early stage of corrosion. However, as the corrosion time increase, AgNWs showed massive fracture after 300s. On the contrary, the AN FEs showed excellent resistance to acid corrosion, and the electrical conductivity remained stable after bearing 1500s corrosion. In addition, it can be found that compared with AgNWs FEs, the chemical corrosion resistance of AgNWs-embedded Nafion FEs is improved, and the resistance change rate is significantly slowed down, which is mainly attributed to that AgNWs embedded layer is protected by the matrix layer, and AgNWs@Au layer is protected by the Au shell, as shown in Figure 3h.

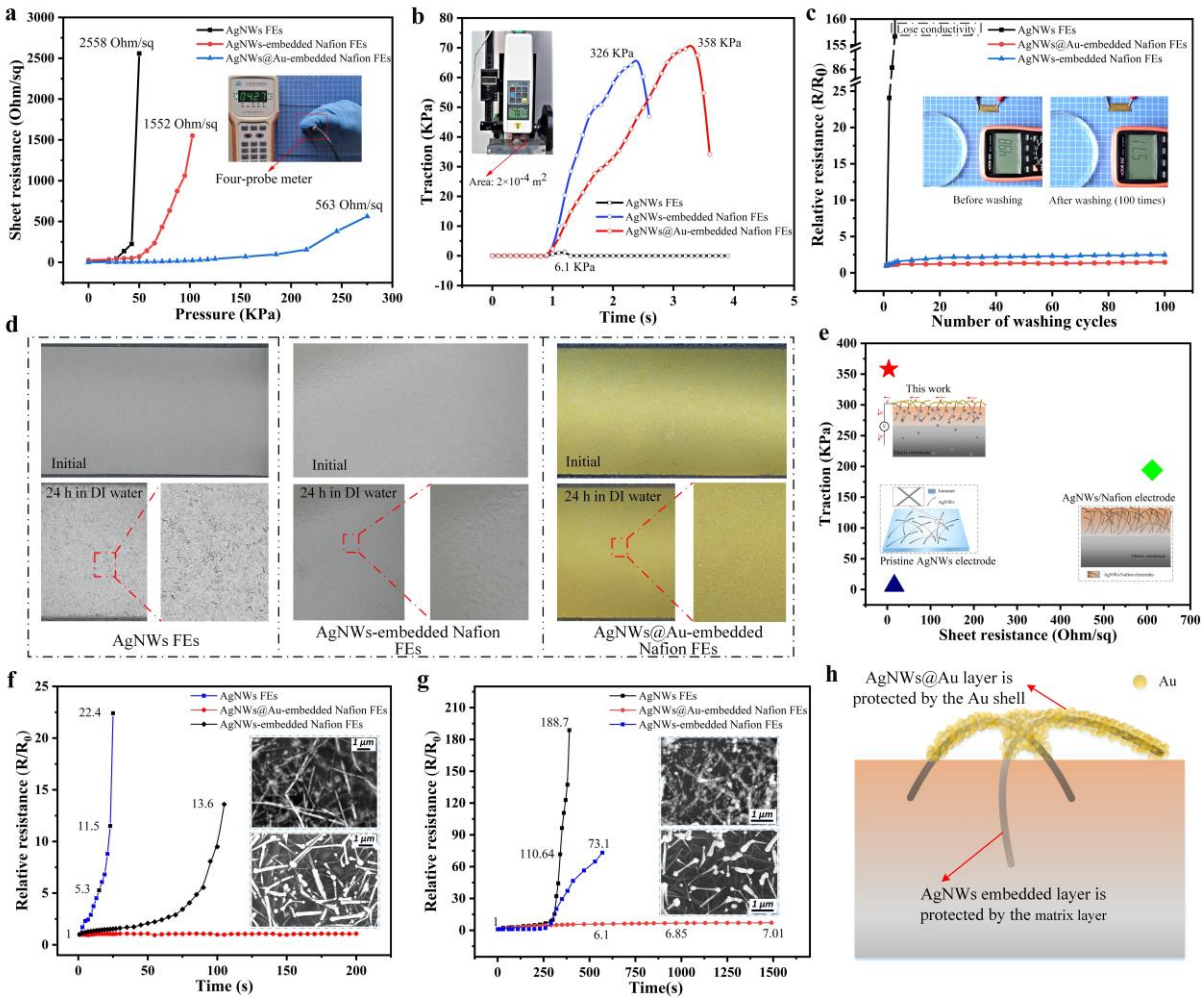

Fig.3. The performance of AN FEs. (a) The sheet resistance changes of FEs polished by 1500P sandpaper under different pressures. (b) The adhesion of FEs. (c) The sheet resistance of FEs after washes. (d) The surface states of FEs before and after immersion in DI water for 24 h. (e) Traction-sheet rasistance in comparison with AgNWs FEs and Nafion/AgNWs FEs. (f) The relative resistance of FEs after H_2O_2 corrosion. (g) The relative resistance of FEs after HCl corrosion. (h) Stability mechanism of AN FEs.

To demonstrate the usefulness of the AN FEs as a part of wearable electronics, a self-powered IFS with dimensions of 30×10 mm was successfully prepared, as shown in Figure 4a. The prepared self-powered IFS has a typical sandwich structure composed of an

ionomer membrane and two AN FEs. The ionomer membrane contains mobile hydrated cations, water and immobile anions. The current mainstream explanation shows that external physical stimulus results in a macroscopic shape or structural change, and the corresponding strain gradient is generated inside the ionomer membrane. Meanwhile, the ions will flow along the gradient direction and through the matrix layer, which generates an electric potential difference in the electrode layer. In addition, humidity changes also cause local anisotropic distribution of the ions inside the ionomer membrane, which will inevitably generate an electrical signal. The signal can directly reflect the change of ambient humidity, as shown in Figure S6 and Figure S7. These two interesting phenomena make the IFS not only have self-powered characteristics without external power, but also can sense the strain and the humidity gradient.

When the prepared self-powered IFS is used as a strain sensor, a VHB tape was attached to its surface for isolating the external environment. Figure 4b shows the voltage signals generated by the strain sensor under strain excitation with different strain. The voltage signal increases from 0.625 mV to 1.15 mV when the bending curvature increases from 53 to 125, showing an almost linear relationship between voltage signal and bending curvature. Meanwhile, the AN FEs are firmly embedded in the matrix layer to form the interfacial layers, which enhances the ion storage capacity of electrodes, thereby improving the voltage amplitude of IFS. Figure 4c shows that the conductivity retention of the AN FEs remained above 95% after 6000 bending cycles, which has good resistance to bending fatigue. In addition, the voltage signals of the self-powered IFS encapsulated with VHB decreased by only 7.6% after exposed to air for 7 days (Fig. 4d). This reason for the slight signal

attenuation is that the strain sensing performance of self-powered IFS degrades as water content decreases. Even with VHB encapsulation, the water content will still gradually volatilize. However, this technical challenge can be overcome by developing better packaging techniques. When the prepared self-powered IFS is used as humidity sensor, it is fixed to the platform to eliminate the strain effect of sensor itself. Figure 4e shows the humidity electrical response curves of the self-powered IFS from 57% RH to other humidity levels. It is clear that the humidification process of the sensor has a higher response speed and response magnitude compared to the dehumidification process. And the greater the humidity gradient is, the stronger the electrical voltage responses. Meanwhile, the voltage change has a characteristic of a slow recovery after a quick rise, which could attribute to the hydrophilic property of the membrane that absorbs water quickly but desorb slowly [27].

Since the self-powered IFS exhibit fast response and high sensitivity to high humidity levels, it can be expected to be used in humidity monitoring. To this end, we explored its application in monitoring the breathing rate of a human. We used a healthy adult male as a volunteer to test his breathing process by blowing into the chamber, in which the self-powered IFS was placed, after sitting for 15 minutes and fast running for 5 minutes separately. Before the breathing test, the sample was first equilibrated at the room humidity environment (about 62% RH). As shown in Figure 4f, self-powered IFS can clearly sense human breathing rate. Additionally, the signal curve shows a rapid rise, then a quick return, corresponding to exhalation and inhalation of a human's breath in the breathing cycle. The maximum of the electrical response is over 12 mV, which is attributed to the numerous droplets in the breathing process rather than the gas form of the water molecules. Meanwhile,

the inhalation process accelerated the air flow around the sensor, which made the sensor quickly dehumidify (the sensor signal recover quickly). To further explore the durability of self-powered IFS. We exposed the sensor to the air for 2 months without any protection, and then monitor the exhalation of the human body. As shown in Figure 4g, after two months, the humidity sensing performance of the sensor has not changed significantly. This satisfactory stability further confirms that the AN FEs can be used in air for a long time.

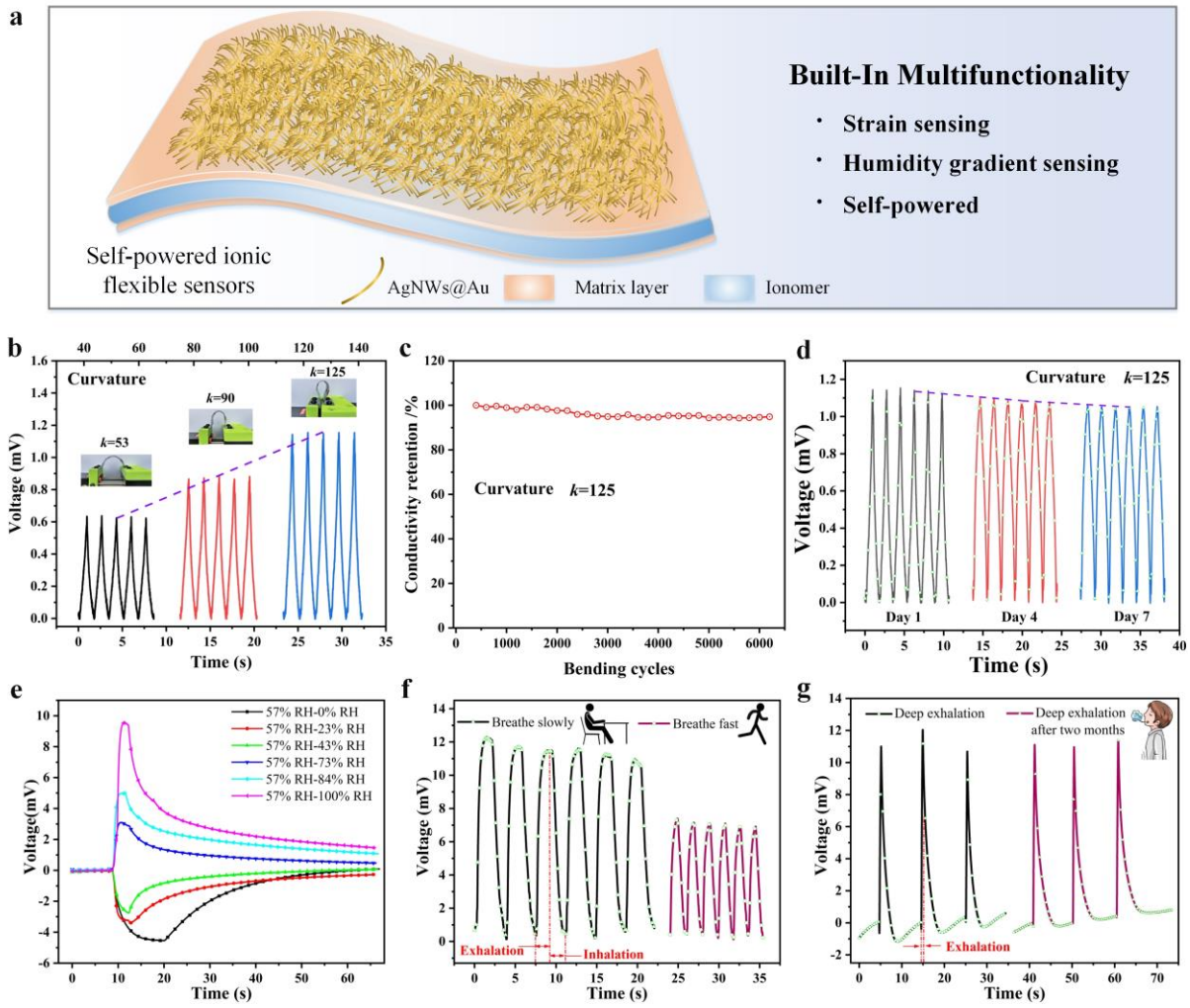

Fig.4. Sensing properties of IFS with AN FEs. (a) A self-powered IFS. (b) The voltage signals generated by the self-powered IFS under strain excitation with different curvatures. (c) The conductivity retention of the AN FEs after bending cycles. (d) The long-time storage stability of the self-powered IFS. (e) The humidity electrical response curves of the self-powered IFS. (f) Breathing

test using the self-powered IFS. (g) The exhalation test using the self-powered IFS after two months.

3. Conclusions

In this work, a rapid, facile, and efficient method was used to form the AN FEs with high conductivity and long-time stability under straightforward conditions. In terms of its simplicity and fastness, the proposed method is unique with lower cost and higher surface area. Through using the spraying and IEP process, the AN FEs were formed with an embedded structure similar to biological hair, the adhesion of which could reach 358 KPa. After 100 washing cycles, the relative change in resistance ($\Delta R/R_0$) was about 14.6%. Meanwhile, high electrical conductivity and remarkable chemical stability were obtained due to the formation of firm joints between AgNWs and Au protective shell. Compared with AgNWs FEs, the sheet resistance of AN FEs can be reduced to 3.7 Ω/□, and the conductivity almost did not change after 200s H_2O_2 corrosion or after 1500s HCl corrosion. Finally, we prepared a self-powered IFS based on AN FEs to achieve dual sensing of mechanical strain and ambient humidity. The prepared sensor shows satisfactory stability and durability, further indicating the potential application of AN FEs in next-generation multifunctional flexible electronic devices.

4. Experimental Section

Materials. Commercially available Nafion® 117 membrane (N117) with a typical thickness of 183 micrometers, which served as an ionomer membrane, was selected and purchased from Dupont™. Nafion solution (20%), which served as the matrix layer, was selected and

purchased from Dupont™. AgNWs (100 nm in diameter with the length range of 100–200 um, concentration at 20 mg mL^{-1} using ethanol as the solvent) were purchased from XFNANO Materials Tech Co., Ltd (Nanjing, China). EtOH (99.5%) and N, N-dimethylacetamide (DMAC) (99%) were purchased from Youso Chemical Technology Co., Ltd (Shandong, China). Auxiliary reagents such as NaOH, H_2O_2 and HCl were obtained from J&K Chemical Inc. (Beijing, China). The deionized water was produced by a hitech-kflow water purification system (Shanghai, China). All the reagents were used as received without further purification.

Fabrication of the solutions. (1) Nafion/DMAC solution: First, the Nafion solution (2 g) was added to the DMAC solution (10 g). Then, after magnetic stirring at 35 °C for 2 h, the Nafion solution was fully dispersed in the DMAC solution, and the Nafion/DMAC solution was obtained. (2) AgNWs/EtOH solution: First, AgNWs (1 mL) was added to EtOH solution (50 mL). Then, the mixed solution was sonicated at 20 °C for 40 min to make the AgNWs were fully dispersed in the EtOH solution. Then the AgNWs/EtOH solution was obtained.

Preparation of the ionomer membrane. Pretreatment: A Nafion membrane with the size of 3.5cm ×3.5cm was cut. It was polished by sandblasting (sand-size: 220#, pressure: 0.4 MPa). Then it was treated successionally with ultrasonic cleaning (60°C, 30 min), acid boiling (hydrochloric acid solution, 2mol l^{-1}, 95°C, 30 min) and DI water boiling (95 °C, 30 min). Post-treatment: The sample was trimmed (3.5×1.5cm) after pretreatment step, then soaked in NaOH solution of 0.6 mol/L for 2 h to conduct cation (Na^+) exchange, and finally put in DI water for standby use.

Fabrication of AN FEs. (a). Nafion/DMAC spraying: a post-treatment Nafion membrane

was placed on a glass plate. Both ends of the Nafion membrane are compressed with two glass plates to prevent swelling or deformation after absorbing the DMAC solution. Then, the spray gun (0.3 mm caliber, 0.15MPa) was placed 3 cm away from the membrane and used to homogeneously disperse the Nafion/DMAC solution (0.8 mL) on it. Meanwhile, Nafion membrane was heated at 120°C using a heating platform. When DMAC was dried, a matrix layer was formed. (b). AgNWs/EtOH spraying: the spray gun (0.3 mm caliber, 0.15MPa) was placed 3 cm away from the membrane with a matrix layer and used to homogeneously disperse the AgNWs/EtOH solution (1.2 mL) on it. Meanwhile, Nafion membrane was heated at 90°C using a heating platform. When EtOH dried, an AgNWs-embedded Nafion electrode was formed. Steps (a) and (b) were repeated to form the electrode layer on the other side. (c). an electroplating set-up was built, which consisted of a titanium anode, DC power supply, and a cathode. The source of Au^{+} was provided by a gold electroplating solution with the mass concentration of 1.2g/L. The electroplating was carried out under 3.5 V around 50s on each side to form the AN FEs.

Characterization. The microstructure of the prepared AN FEs was characterized by a ZEISS Sigma 500 field emission scanning electron microscope. The resistance of the sample was measured by a Yisheng Victor Tech Co., Ltd. VICTOR 86E multimeter (Shenzhen, China) and a Jingge Electronics Co., Ltd. M3 four-probe meter (Suzhou, China). Aidebao^{TM} HP tension gauge was used to test the adhesion. The strain-sensing performance of the sensor was tested using a self-made machine that can bend the sample to various bending curvatures (Fig. S4). The changes of the sensing voltage signal were recorded using a signal acquisition card in real time (NI USB-6001). The humidity sensing performance of the sensor was tested

using a self-made humidity sensing platform, which was able to generate a variety of humidity levels (Fig. S5). Meantime, a signal acquisition card (NI USB-6001) was used to record the changes of the sensor voltage signal in real time.

ASSOCIATED CONTENT

The Supporting Information is available free of charge on the ACS Publications website. Figures S1, the effects of AgNWs density on electrode properties and sensing performance (Figure S2), the effects of IEP time on electrode properties (Figure S3), The strain-sensing platform (Figure S4), Humidity sensing platform (Figure S5), Mechanism of IFS strain-sensing (Figure S6), Mechanism of IFS humidity sensing (Figure S7) (**PDF**). Repeated washing cycles (Video S1) (**MP4**). H2O2 corrosion (Video S2) (**MP4**).

Corresponding Author

* Corresponding authors: Yanjie Wang, Email: yj.wang1985@gmail.com

Author Contributions

The manuscript was written through contributions of all authors. All authors have given approval to the final version of the manuscript. ‡These authors contributed equally: Chun Zhao, Yanjie Wang.

Acknowledgements

This research was supported by the National Natural Science Foundation of China (51975184, 52075411, and 52105573), the Fundamental Research Funds for the Central Universities (B210202124), the Changzhou Sci &Tech Program (CE20215051), the National Key

Research and Development Program of China (2020YFB1312900), and Postgraduate Research & Practice Innovation Program of Jiangsu Province (KYCX22_0672). The authors gratefully acknowledge the supports.

References

[1]. Zhao, C., Wang, Y., Tang, G., Ru, J., Zhu, Z., Li, B., Guo, C. F., Li, L., Zhu, D., Ionic Flexible Sensors: Mechanisms, Materials, Structures, and Applications. Adv. Funct. Mater. 2022, 2110417

[2]. Y. Wang, G. Tang, C. Zhao, D. Mei, et al. The effects of contact area on pressure sensing of ionic polymer metal composite sensor with a soft substrate. Smart Mater. Struct. 2022, 31, 065013.

[3]. Wang, Y., Liu, Q., Zhang, J., Hong, T., Sun, W., Tang, L., Arnold, E., Suo, Z., Hong, W., Ren, Z., Guo, C. F., Giant Poisson's Effect for Wrinkle-Free Stretchable Transparent Electrodes. Adv. Mater. 2019, 31, 1902955.

[4]. Wang Y., Liu J., Zhu Y., Zhu D., Chen H., Formation and Characterization of Dendritic Interfacial Electrodes inside an Ionomer. ACS Appl. Mater. Interfaces 2017, 9, 36, 30258–30262.

[5]. Guo C., Chen Y., Tang L., Wang F., Ren Z., Enhancing the Scratch Resistance by Introducing Chemical Bonding in Highly Stretchable and Transparent Electrodes. Nano Lett. 2016, 16, 1, 594–600.

[6]. Lu, H., Zhang, D., Cheng, J., Liu, J., Mao, J. and Choy, W.C.H., Locally Welded Silver Nano-Network Transparent Electrodes with High Operational Stability by a Simple Alcohol-Based Chemical Approach. Adv. Funct. Mater., 2015, 25: 4211-4218.

[7]. Li Q., Deng M., Zhang S., Zhao D., Jiang Q., Guo C., Zhou Q., Liu W., Synergistic enhancement of thermoelectric and mechanical performances of ionic liquid LiTFSI modulated PEDOT flexible films. J. Mater. Chem. C, 2019,7, 4374-4381.

[8]. Mian J., Chen S., Liu H., Zhang X., Low-temperature nanowelding ultrathin silver nanowire sandwiched between polydopamine-functionalized graphene and conjugated polymer for highly stable and flexible transparent electrodes. Chemical Engineering Journal 2018, 345, 260–270.

[9]. H., Jeong, Y., Noh, S., H., Ko, D., Lee, Flexible resistive pressure sensor with silver nanowire networks embedded in polymer using natural formation of air gap. Composites Science and Technology 2019, 174, 50–57.

[10]. J. Ru, C. Bian, Z. Zhu, Y. Wang, J. Zhang, T. Horiuchi, et al. Controllable and durable ionic electroactive polymer actuator based on nanoporous carbon nanotube film electrode. Smart Mater. Struct. 2019, 28, 085032.

[11]. S.-R. Kim, J.-H. Kim, J.-W. Park. Wearable and Transparent Capacitive Strain Sensor with High Sensitivity Based on Patterned Ag Nanowire Networks. ACS Appl. Mater. Interfaces 2017, 9, 31, 26407–26416.

[12]. Liu X., Li D., Chen X., Lai W., Huang W., Highly Transparent and Flexible All-Solid-State Supercapacitors Based on Ultra-Long Silver Nanowire Conductive Networks. ACS Appl. Mater. Interfaces 2018, 10, 38, 32536–32542.

[13]. B. Zhang, W. Li, Y. Yang, C. Chen, C.-F. Li, K. Suganuma. Fully embedded CuNWs/PDMS conductor with high oxidation resistance and high conductivity for stretchable electronics. J Mater Sci. 2019, 54:6381–6392.

[14]. H. Zhang, Y. Yang, T. Liu, H. Chang. Boosting the Power-Generation Performance of Micro-Sized Al-H_2O_2 Fuel Cells by Using Silver Nanowires as the Cathode. Energies 2018, 11, 2316.

[15]. Zhu Y., Hu Y., Zhu P., Zhao T., Liang X., Sun R., Wong C., Enhanced oxidation resistance and electrical conductivity copper nanowires–graphene hybrid films for flexible strain sensors. New J. Chem., 2017, 41, 4950.

[16]. I., Hong, S., Lee, D., Kim, H., Cho, Y., Roh, H., An, S., Hong, S., H., Ko, S., Han, Study on the oxidation of copper nanowire network electrodes for skin mountable flexible, stretchable and wearable electronics applications. Nanotechnology 2019, **30,** 074001.

[17]. Quan Y., Wei X., Xiao L., Wu T., Pang H., Liu T., Huang W., Wu S., Li S., Chen Z., Highly sensitive and stable flexible pressure sensors with micro-structured electrodes. Journal of Alloys and Compounds 2017, 699, 824-831.

[18]. Wang Y., Wang J., Hao M., Li B., Zhu Z., Gou X., Li L., Rapid preparation of a Nafion/Ag NW composite film and its humidity sensing effect. RSC Adv., 2020, 10, 27447.

[19]. Y., Kim, J., Kim, Silver nanowire networks embedded in urethane acrylate for flexible capacitive touch sensor. Applied Surface Science 2016, 363, 1–6.

[20]. Ding S., Jiu J., Gao Y., Tian Y., Araki T., Sugahara T., Nagao S., Nogi M., Koga H., Suganuam K., Uchida H., One-Step Fabrication of Stretchable Copper Nanowire Conductors by a Fast Photonic Sintering Technique and Its Application in Wearable Devices. ACS Appl. Mater. Interfaces 2016, 8, 6190−6199.

[21]. B. Zhang, W. Li, M. Nogi, C. Chen, Y. Yang, T. Sugahara, H. Koga, K. Suganuma. ACS Applied Materials & Interfaces 2019 11 (20), 18540-18547.

[22]. Lu, H., Zhang, D., Cheng, J., Liu, J., Mao, J. and Choy, W.C.H., Locally Welded Silver Nano-Network Transparent Electrodes with High Operational Stability by a Simple Alcohol-Based Chemical Approach. Adv. Funct. Mater., 2015, 25: 4211-4218.

[23]. S., Lim, J., Oh, B., Yoo, C., Han, B., Lee, M., Oh, J., Kim, Transparent and stretchable capacitive pressure sensor using selective plasmonic heating-based patterning of silver nanowires. Applied Surface Science 2021, 561, 149989.

[24]. S., Tseng, C-C., Huang, Investigation of interactions between high pulsed ultraviolet lasers and composite graphene/AgNWs films. Applied Surface Science 2021, 570, 151060.

[25]. R., T., Ginting, M., M., Ovhal, J-W., Kang, A novel design of hybrid transparent electrodes for high performance and ultra-flexible bifunctional electrochromic-supercapacitors. Nano Energy 2018, 53, 650–657.

[26]. Zhang H., Tian Y., Wang S., Huang Y., Wen J., Hang C., Zheng Z., Wang C., Highly stable flexible transparent electrode via rapid electrodeposition coating of Ag-Au alloy on copper nanowires for bifunctional electrochromic and supercapacitor device. Chemical Engineering Journal 2020, 399, 125075.

[27]. Y. Wang, G. Tang, C. Zhao, K. Wang, J. Wang, J. Ru, J. Sheng, L. Chang, L. Li. Experimental investigation on the physical parameters of ionic polymer metal composites sensors for humidity perception. Sensors & Actuators: B. Chemical 2021, 345, 130421.